Supplementary Information (SI) for ChemComm.
This journal is © The Royal Society of Chemistry 2024

Supporting Information

Small-sized Starch Nanoparticles for Efficient Penetration of Plant Cells

Yongxian Chen[a], Simin Jiang[b], Yang Wang[a], Fuxue Zhang[b], Liu Wang[a], Li Zhao[c], SiYu Liu[b], JunJun Tan[d], Staffan Persson[a], Bo Sun[e]*, Junsheng Chen[b]*, Andreas Blennow[a]*

1. Materials and Methods

1.1 Materials and Chemical reagents

High amylose maize starch (G50) was sourced from Penford Australia Ltd., NSW, Australia. 2,2,6,6-Tetramethylpiperidine 1-oxyl (TEMPO), sodium bromide (NaBr), sodium hypochlorite solution (6-14% active chlorine)(NaClO), ethanol (EtOH), Nile blue a (NB), tween 80, N-(3-Dimethylaminopropyl)-N'-ethylcarbodiimide hydrochloride (EDCl), N-Hydroxysuccinimide (NHS) were purchased from Sigma-Aldrich (Denmark). The pUBQ10::acyl-YFP Arabidopsis marker line was reported before[1].

1.2 Preparation of fluorescent small-sized starch nanoparticles (NB@G50-NPs)

The NB@G50-NPs were produced through an amidation method involving EDC/NHS. The preparation process was divided into three phases: selective oxidation of G50-NPs, primary preparation of NB@G50-NPs, and purification of NB@G50-NPs.

Selective oxidation of G50-NPs:

Small-sized starch nanoparticles (G50-NPs) were used as the starting material, prepared from 2% (w/v) G50 according to our previous study[2]. NaBr (160 mg) and TEMPO (16 mg) were added to 35 mL of G50-NPs and dissolved completely[3] and pH adjusted to 10. Next, 3 mL of NaClO was added to the system, and the mixture was stirred at a constant speed of 400 RPM for 2 h. The reaction was terminated by adding 10 mL of ethanol (EtOH), and pH adjusted to 6. The EtOH was removed by centrifugation at 3000 g. The sediments were re-dispersed in 10 mL of 0.1% (w/v) Tween 80 for the subsequent step.

Primary preparation of NB@G50-NPs:

EDCl and NHS (2 mg each) were added to the oxidized G50-NPs and stirred at 400 RPM overnight[4]. Ten mL of purified NB was added to 2 mL of the overnight sample

and stirred at 300 RPM for 2 h. In this step, 10 mL of purified NB was filtered using a 0.22 µm hydrophilic filter from 5 mg of NB powder dissolved in 10 mL of Milli-Q water.

Purification of NB@G50-NPs:

Purified NB@G50-NPs were obtained after the free fluorescent dye (NB) was removed by ultrafiltration centrifugation (10 kDa MWCO) until the filtrate was transparent and the absorbance was almost zero.

1.3 Transmission electron microscopy (TEM)

To assess the size and morphological differences between synthesized NB@G50-NPs and G50-NPs, the NB@G50-NPs were visualized with a LVEM 5 transmission electron microscope (TEM) (Delong instruments, Montreal Quebec, Canada). Statistical analysis of NB@G50-NPs and G50-NPs sizes was performed on at least 300 particles observed in the TEM images.

1.4 Detection of absorbance and emission Spectra features

All absorbance experiments were carried out using a 1 cm cuvette with a Cary 300 UV-Vis Spectrophotometer (Agilent Technologies, USA). All emission experiments were performed using a 1 cm cuvette with an FT 300 (Xe) instrument (Picoquant, Berlin, Germany). For emission experiments, the excitation wavelength was 540 nm and both NB and NB@G50-NPs were dissolved in Milli-Q water. For fluorescence quantum yield and lifetime experiments, NB was dissolved in methanol (FQY=27%) as the reference[5], while the NB sample and NB@G50-NPs were dissolved in Milli-Q water. For the stability test, NB@G50-NPs were aliquoted into different pH buffers for 0 and 72 h. Citrate buffer (pH 3-5), phosphate buffer (pH 6-8), and Tris-HCl buffer (pH 9-10) were used in this study.

1.5 Theoretical calculations of NB@G50-NPs

In the current work, all the theoretical calculations were executed in Gaussian 09 software package[6]. The most stable structure of NB and NB@G50-NPs in ground state (S_0) were optimized without constraint by using the density functional theory (DFT) method. The Becke′s three-parameter hybrid exchange function with the Lee-Yang-Parr gradient-corrected correlation functional (B3LYP)[7] and the 6-31G (d,p)[8] basis set were employed throughout. Vibrational frequencies were further calculated to confirm that the optimized structures are global minima on S_0 potential energy surface.

Vertical excitation energies and corresponding oscillator strengths were calculated with TDDFT method at the optimized ground state structure with six low-lying absorption transitions. The B3LYP functional and tzvp[9] basis set were employed. For both the structure optimizations and vertical energy calculations, the polarization continuum model (PCM) using the integral equation formalism variant (IEF-PCM)[10,11] was employed to account for the effect of water.

1.6 The calculation of fluorescent dye concentration in NB@G50-NPs

The calculation of the fluorescent dye concentration was based on the Beer–Lambert law.

$$A = \varepsilon cL$$

A: absorbance

ε: Molar extinction coefficient of Nile blue a, 68,000 $M^{-1}cm^{-1}$ in this study.

L: Path length of the light through the solution, 1 cm in this study.

1.7 Live cell imaging in Arabidopsis based on NB@G50-NPs.

The chlorine gas sterilized Arabidopsis seeds were grown on 1/2 Murashige and Skoog (MS) media containing 2.56 mM MES, 1% (w/v) sucrose (pH 5.7-5.8), and 0.8% (w/v) agar. The plates were vernalized at 4°C in darkness for 2 days and then transferred to growth chambers with 16 hours of light at 21°C and 8 hours of dark at 18 °C. The 7-day-old seedlings were used for further imaging. The seedlings were immersed in 3 mL of a solution of NB@G50-NPs and NB (diluted a solution with an absorbance of 0.1 by 500-fold) in a 6-well culture plate at room temperature for 30 minutes. They were then rinsed three times with Milli-Q water before imaging with a Confocal Laser Scanning Microscope (CLSM, Leica Stellaris 8 with a 20X 1.25 objective). Two excitation wavelengths were used: 514 nm for YFP and 631 nm for Nile Blue A. Z-stack imaging was captured with a 0.7 µm step size in the maturation zone of the roots. The imaging was processed and analyzed in ImageJ[12]. Moreover, 10 slices of the Z-stacks, taken 7 µm beneath the plasma membrane focal plane, were used to generate average intensity Z-projection images. These maximum intensity Z-projection images were used for quantifying fluorescence intensity. Quantification of fluorescence intensity (Integrated Density, IntDen) was performed on 5 biological replicates (n = 15, where n represents regions of interest) for both NB and NB@G50-NPs.

1.8 Statistical analysis

All experiments were performed in triplicates. The statistical analysis was performed using lmerTest (1)[13] package in R (2)[14]

Figures captions

Fig. S1 The size and morphology of the prepared NB@G50-NPs based on TEM.

Fig. S2 Purification of NB@G50-NPs was based on centrifugal ultrafiltration.

Fig. S3 Lifetime fluorescence of NB@G50-NPs and NB.

Fig. S4 NB@G50-NPs likely penetrate plant cells by endocytosis.

Fig .S5 The live cell imaging of NB in Arabidopsis roots.

Fig. S6 The live cell imaging of NB@G50-NPs in Arabidopsis roots.

Fig. S7 The proposed absorption pathways of NB@G50-NPs in plants.

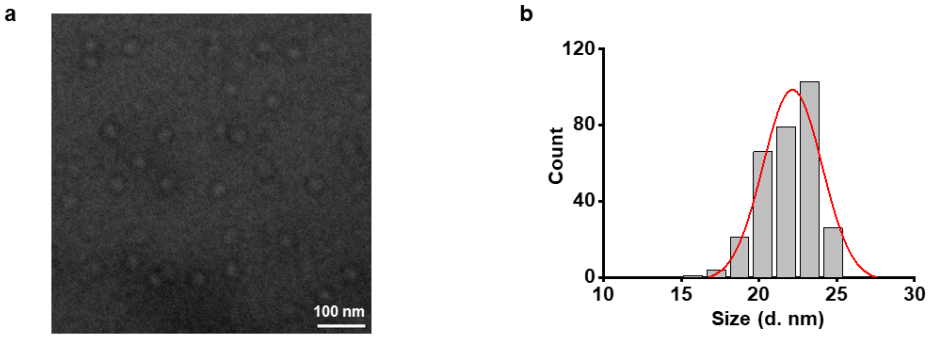

Fig. S1 Size and morphology of the prepared NB@G50-NPs based on TEM. TEM images of NB@G50-NPs (a) and TEM-based size distributional analysis of and NB@G50-NPs (b).

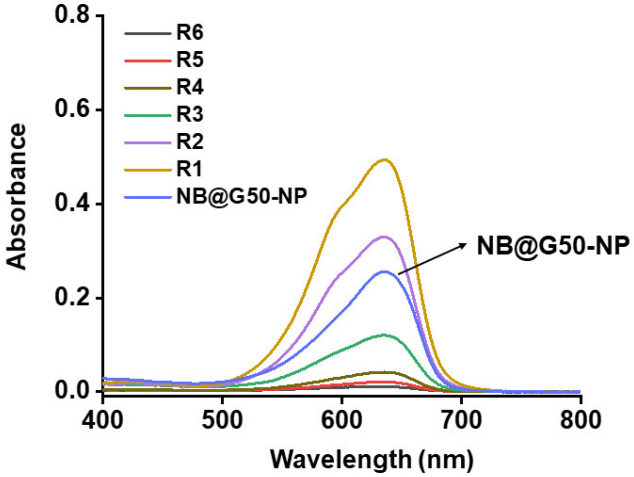

Fig. S2 Purification of NB@G50-NPs was based on centrifugal ultrafiltration. R1/R2/R3/R4/R5/R6: results after the first/sixth rinse with 0.1% (w/v) Tween 80 following ultrafiltration centrifugation.

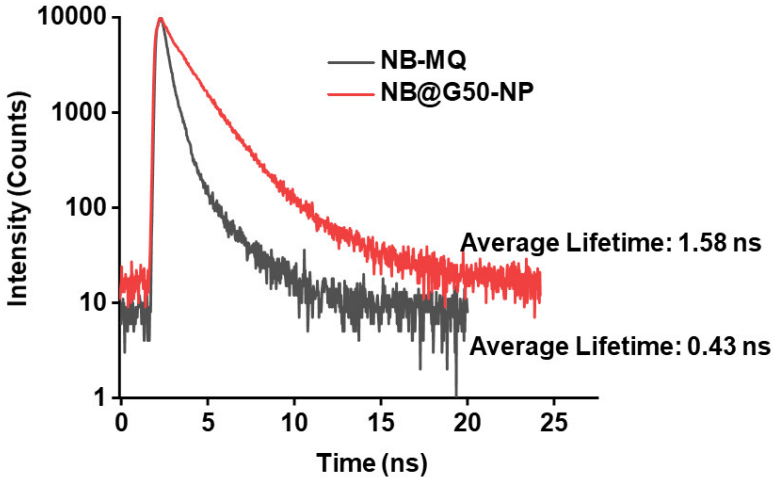

Fig. S3 Lifetime fluorescence of NB@G50-NPs and NB.

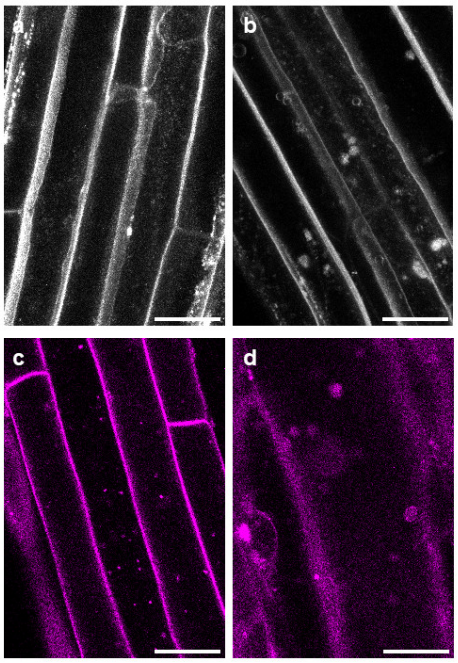

Fig. S4. NB@G50-NPs likely penetrate plant cells by endocytosis. (a, c) FM4-64 (2.8 μM) and NB@G50-NPs (2.9 nM), each applied separately to Arabidopsis roots for 30 minutes. (b) Combined application of BFA (50 μM) and FM4-64 (2.8 μM) on Arabidopsis roots for 30 min. (d) Combined application of BFA (50 μM) and NB@G50-NPs (2.9 nM) on Arabidopsis roots for 30 min. Scale bar: 20 μm.

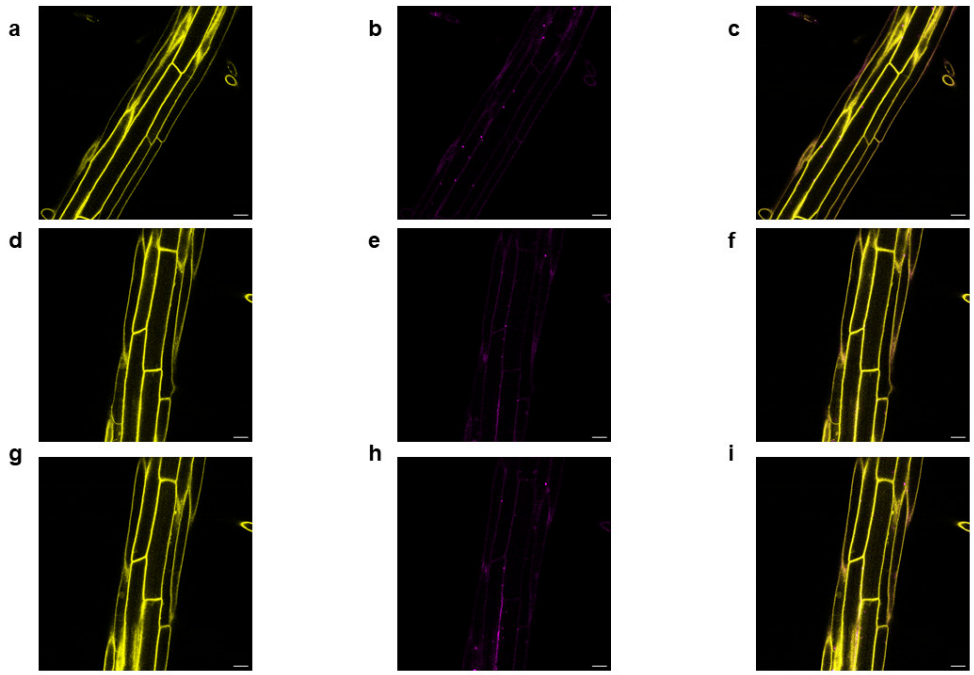

Fig. S5 The live cell imaging of NB in Arabidopsis roots. a-i) Representative images of NB uptake into 7-day-old Arabidopsis root cells. a, d and g) pUBQ10::acyl-YFP; b, e and h) NB; c, f and i) Merged image of NB and pUBQ10::acyl-YFP.

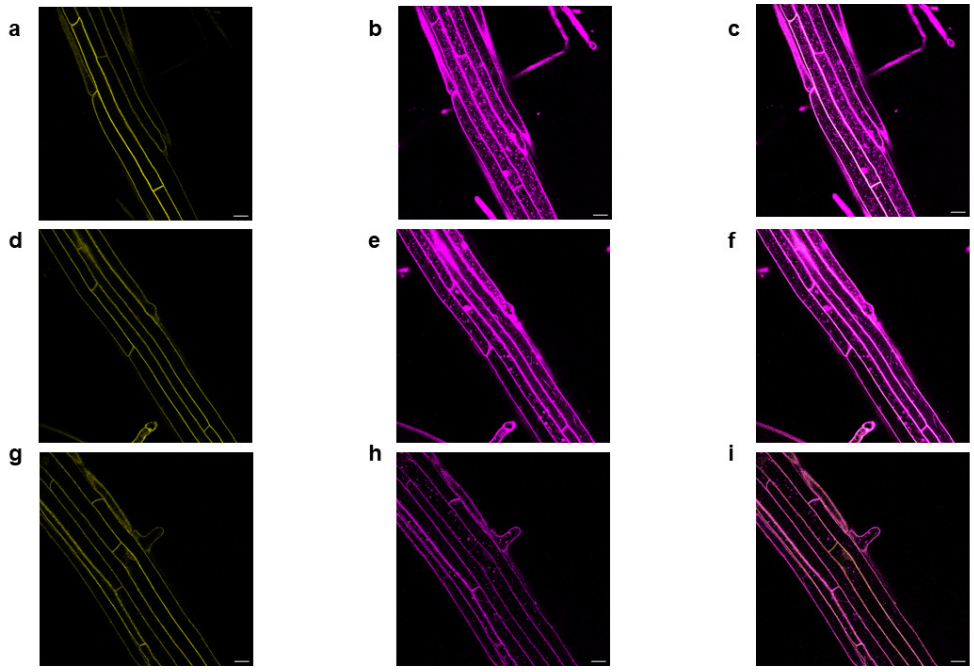

Fig. S6 The live cell imaging of NB@G50-NPs in Arabidopsis roots. a-i) Representative images of NB@G50-NPs uptake into 7-day-old Arabidopsis root cells. a, d and g) pUBQ10::acyl-YFP; b, e and h) NB@G50-NPs; c, f and i) Merged image of NB@G50-NPs and pUBQ10::acyl-YFP

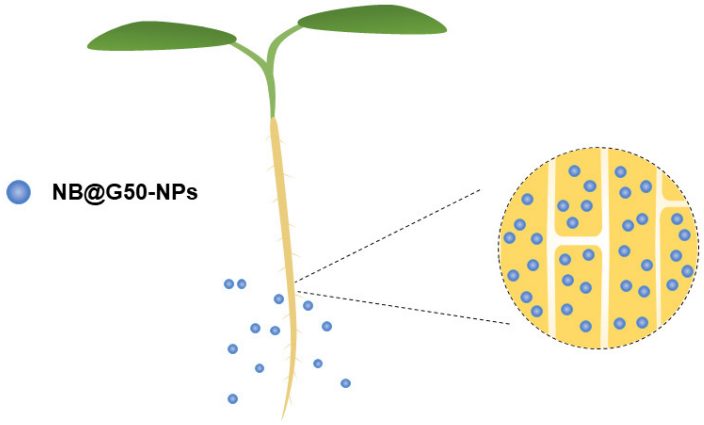

Fig. S7 The proposed absorption pathways of NB@G50-NPs in plants

References

1 Willis, L. *et al.* Cell size and growth regulation in the Arabidopsis thaliana apical stem cell niche. *Proceedings of the National Academy of ences* **113**, 201616768 (2016).

2 Chen, Y. *et al.* Green preparation of small-sized starch nanoparticles using nanoprecipitation. *Food Hydrocolloids* **153**, doi:10.1016/j.foodhyd.2024.109974 (2024).

3 Isogai, A. TEMPO-catalyzed oxidation of polysaccharides. *Polymer Journal*, 54 (2022).

4 Sam, S. *et al.* Semiquantitative study of the EDC/NHS activation of acid terminal groups at modified porous silicon surfaces. *Langmuir the Acs Journal of Surfaces & Colloids* **26**, 809-814 (2010).

5 Sens, R. & Drexhage, K. H. Fluorescence quantum yield of oxazine and carbazine laser dyes. *Journal of Luminescence* **24**, 709-712 (1981).

6 M., J. F., G *et al.* Gaussian 09, Revision A. 1; Gaussian. (2009).

7 Lee, C., Yang, W. & Parr, F. R. G. Results obtained with the correlation energy density functionals of Becke and Lee, Yang and Parr. *Physiological Reviews* (1988).

8 Rassolov, V. A., Pople, J. A., Ratner, M. A. & Windus, T. L. 6-31G* basis set for atoms K through Zn. *The Journal of Chemical Physics* (1998).

9 Schäfer, A., Huber, C. & Ahlrichs, R. Fully optimized contracted Gaussian basis sets of triple zeta valence quality for atoms Li to Kr. *J.chem.phys* **100**, 5829-5835 (1994).

10 Miertu, S., Scrocco, E. & Tomasi, J. Electrostatic interaction of a solute with a continuum. A direct utilizaion of AB initio molecular potentials for the prevision of solvent effects. *Chemical Physics* **55**, 117-129 (1981).

11 Cammi, R. & Tomasi, J. Remarks on the Use of the Apparent Surface Charges (ASC) Methods in Solvation Problems: Iterative Versus Matrix-Inversion Procedures and the Renormalization of the Apparent Charges. *Journal of Computational Chemistry* **16**, 1449-1458 (1995).

12 Schindelin, J. *et al.* Fiji: an open-source platform for biological-image analysis. *Nature methods*, 9 (2012).

13 Kuznetsova, A., Brockhoff, P. B. & Christensen, R. H. B. lmerTest Package: Tests in Linear Mixed Effects Models. (2019).

14 Team, R. D. C. R: A Language and Environment for Statistical Computing. R Foundation for Statistical Computing:Vienna, Austria. *Computing* **14**, 12-21 (2009).